# Edge ion heating by launched high harmonic fast waves in the National Spherical Torus Experiment

T.M. Biewer,* R.E. Bell, S.J. Diem, C.K. Phillips, and J.R. Wilson
*Princeton Plasma Physics Laboratory, Princeton, NJ 08543*

P.M. Ryan
*Oak Ridge National Laboratory, Oak Ridge, TN 37831*
(Dated: January 6, 2005)

A new spectroscopic diagnostic on the National Spherical Torus Experiment (NSTX) [J. Spitzer, M. Ono, *et al.*, Fusion Technology **30**, 1337 (1996)] measures the velocity distribution of ions in the plasma edge simultaneously along both poloidal and toroidal views. An anisotropic ion temperature is measured during high power High Harmonic Fast Wave (HHFW) rf heating in helium plasmas, with the poloidal ion temperature roughly twice the toroidal ion temperature. Moreover, the measured spectral distribution suggests that two populations of ions are present and have temperatures of typically 500 eV and 50 eV with rotation velocities of -50 km/s and -10 km/s, respectively (predominantly perpendicular to the local magnetic field). This bi-modal distribution is observed in both the toroidal and poloidal views (for both $He^{+}$ and $C^{2+}$ ions), and is well correlated with the period of rf power application to the plasma. The temperature of the hot component is observed to increase with the applied rf power, which was scanned between 0 and 4.3 MW. The 30 MHz HHFW launched by the NSTX antenna is expected and observed to heat core electrons, but plasma ions do not resonate with the launched wave, which is typically at $> 10^{th}$ harmonic of the ion cyclotron frequency in the region of observation. A likely ion heating mechanism is parametric decay of the launched HHFW into an Ion Bernstein Wave (IBW). The presence of the IBW in NSTX plasmas during HHFW application has been directly confirmed with probe measurements. IBW heating occurs in the perpendicular ion distribution, consistent with the toroidal and poloidal observations. Calculations of IBW propagation indicate that multiple waves could be created in the parametric decay process, and that most of the IBW power would be absorbed in the outer 10 to 20 cm of the plasma, predominantly on fully stripped ions. These predictions are in qualitative agreement with the observations, and must be accounted for when calculating the energy budget of the plasma.

## I. INTRODUCTION

The interaction of rf waves with magnetically confined plasmas is an important but complex issue in the plasma physics community. Radio frequency heating and current drive systems are major components of present fusion-grade experiments, such as the National Sperical Torus Experiment (NSTX)[1], DIII-D[2], Alcator C-Mod[3], and the Joint European Torus (JET)[4]. Moreover, rf heating and current drive are expected to be reliable tools in future burning plasma experiments, such as the International Tokamak Experimental Reactor (ITER)[5, 6] or the Fusion Ignition Research Experiment (FIRE)[7]. In NSTX, the High Harmonic Fast Wave (HHFW)[8] launched by the rf antenna is expected (and observed) to heat core electrons, but for the plasma parameters discussed here, the plasma ions should be unaffected[9]. However, thermal ion heating at the edge of the plasma is observed when rf power is applied[10]. This discrepancy between the intent and the manifestation of rf power in the plasma needs to be understood, so that an accurate understanding of the physics of the interaction between rf waves and fusion-plasmas can be achieved.

The National Spherical Torus Experiment (NSTX) is a large, magnetically confined plasma device[11]. NSTX has a major radius of $R \sim 0.85$ m and a minor radius of $a \sim 0.65$ m, for an aspect ratio of $R/a \sim 1.3$. The cross-section of NSTX plasmas can be highly shaped, with an upper-single-, lower-single-, or double-null diverted configuration, as well as an inner- or outer-wall limited configuration. For the discharges discussed here, the plasma elongation is typically 1.77, with a triangularity of 0.45 at the lower x-point. The results presented here are primarily lower-single-null configured plasmas, with an on-axis toroidal magnetic field of $\sim 0.4$ T and a plasma current of 500 kA. The Thomson scattering (TS)[12] measured on-axis electron temperature varies with the amount of applied rf power, but a value of $T_e(0) \leq 2$ keV is typical, with an on-axis electron density of $n_e(0) \sim 2 \times 10^{19}$ m$^{-3}$. Pulse lengths for these discharges are $\sim 600$ ms.

Auxiliary heating can be applied to NSTX plasmas by neutral beam injection (NBI) or by rf heating. The 12-element coupler of the 30 MHz HHFW rf system on NSTX can be phased either to heat the plasma or to drive current[13]. In the experiments described here, NBI was used in a few discharges (in 7 ms bursts spaced by 50 ms) to gain measurements of the ion temperature profile into the core of the plasma through charge exchange and recombination spectroscopy (CHERS). These bursts of NBI are short compared to the beam slowing-down-time in the plasma ($\sim$ 30 ms), and hence the plasma experiences rf auxiliary heating predominantly. The ma-

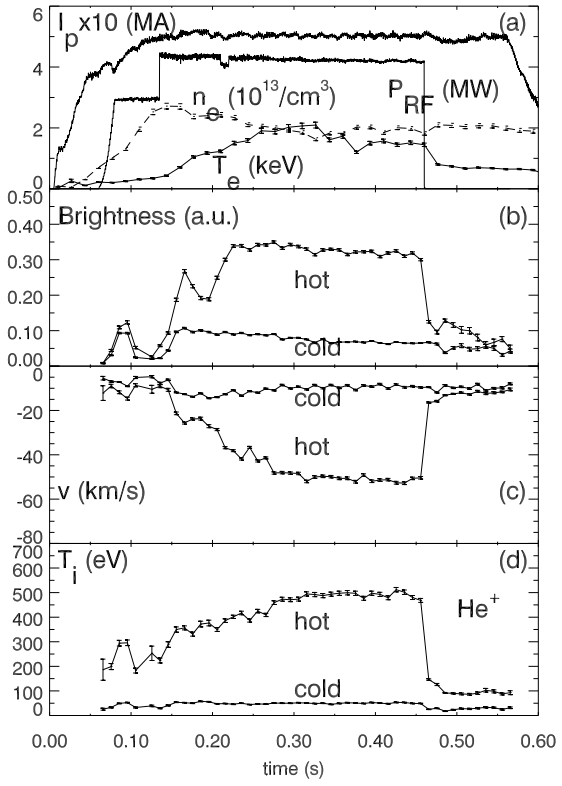


FIG. 1: Time evolution of NSTX Shot 110144, showing (a) $I_p$, $T_e$, $n_e$, and $P_{RF}$ and the hot and cold components of poloidally measured $He^+$ (b) brightness, (c) velocity, and (d) temperature at a tangency radius of 146 cm.

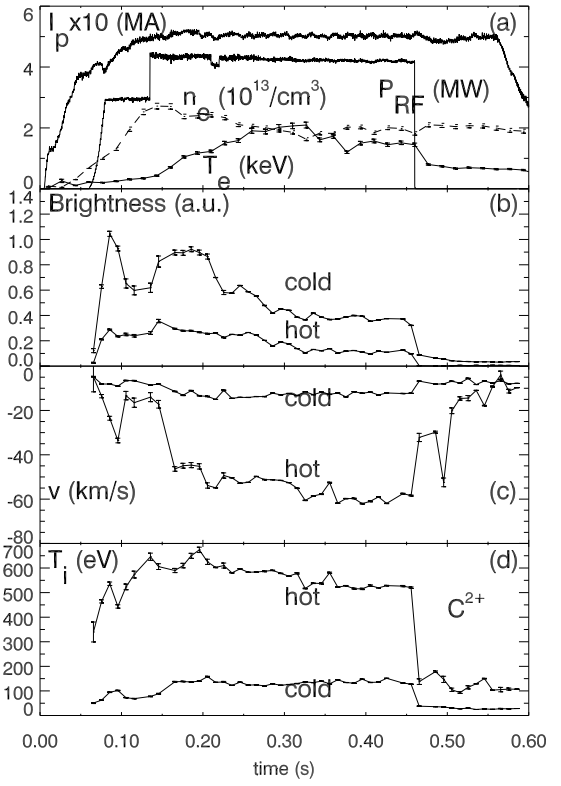


FIG. 2: Time evolution of NSTX Shot 110144, showing (a) $I_p$, $T_e$, $n_e$, and $P_{RF}$ and the hot and cold components of poloidally measured $C^{2+}$ (b) brightness, (c) velocity, and (d) temperature at a tangency radius of 146 cm.

jority of discharges had no NBI pulses whatsoever.

A new edge rotation diagnostic (ERD)[14] was used to augment the CHERS measurements of the ion dynamics in the edge plasma. Whereas the NSTX CHERS system measures the light (due to intrinsic emission and to charge exchange) from $C^{5+}$ ions (5291 Å), predominantly in the bulk plasma, the ERD measures light from intrinsic emission of $C^{2+}$ (4650 Å), $C^{3+}$ (4658 Å), and $He^+$ (4685 Å) in the edge plasma. These spectral lines are measured simultaneously along sight lines in both the poloidal and toroidal directions, with a 10 ms integration period. Measurement chords of the ERD cover the outer 20 cm of the plasma, with $\sim 3$ cm spacing.

## II. OBSERVATIONS

A variety of effects are observed when rf power is applied to the plasma. As shown in Fig. 1 (a) and Fig. 2 (a), the on-axis electron temperature is observed to rise, when the rf antenna is broadcasting. The electron temperature remains high until MHD activity begins. At that point $T_e$ is reduced but still elevated, especially compared to the electron temperature after the rf has terminated. This electron heating is expected, since calculations show that the electrons absorb energy efficiently from the HHFW[9]. The rf frequency is about the $10^{th}$ harmonic of the helium cyclotron frequency at the discharge center and the ions are nowhere fundamentally resonant with the HHFW so the ion energy absorption efficiency is calculated to be negligible. Fig. 3 shows a comparison between the measured electron (from TS) and ion (from CHERS) temperature profiles during HHFW application. Calculated profiles of the RF energy absorption for electrons and ions are shown in Fig. 4. These calculations were done using the linear full-wave field solver TORIC, which has been modified to be valid in the HHFW regime[15].

Also shown in Fig. 3 are the ERD measured edge $He^+$ ion temperature profiles. Elevated edge ion temperatures are observed in NSTX during the application of HHFW[10, 16, 17]. When the rf is applied, edge ion temperatures greatly exceed edge electron temperatures. These enhanced edge ion temperatures can easily be seen in the raw ERD data, as shown in Fig. 5. The spectra of $He^+$ and $C^{2+}$ are best fit with double-Gaussian distribution functions, indicating the presence of both hot and cold components in the distributions at the same ra-

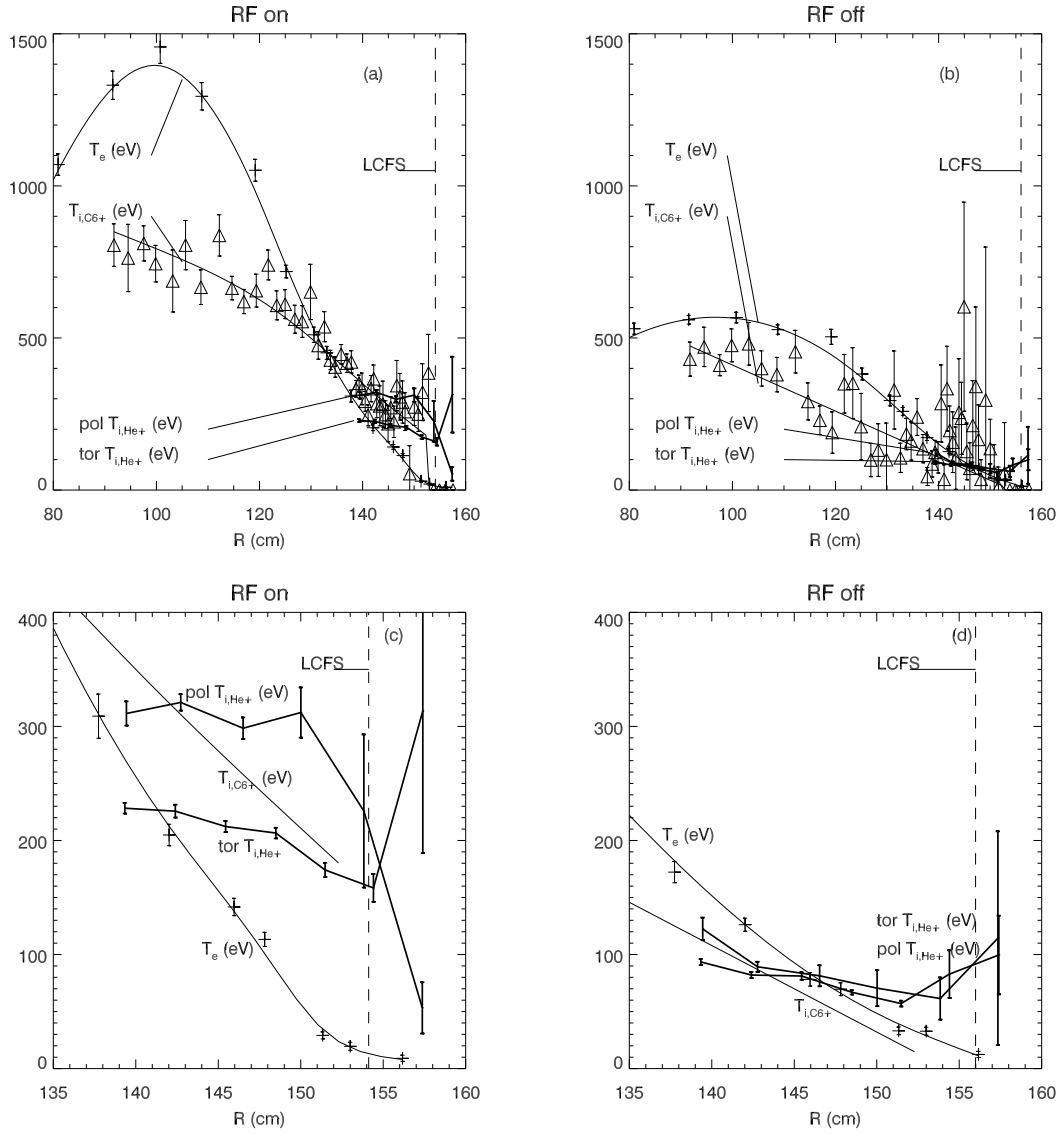


FIG. 3: Radial profiles of Thomson scattering measured electron temperature, CHERS measured $C^{6+}$ ion temperature, and ERD measured $He^+$ ion temperatures (a) during the application of 2.8 MW of HHFW power in shot 112310 at 275 ms and (b) with no rf at 175 ms. Edge radial profiles of $T_e$, CHERS spline fit to measured $C^{6+}T_i$, and ERD measured $He^+T_i$ (c) during the application of 2.8 MW of HHFW power in shot 112310 at 275 ms and (d) with no rf at 175 ms.

dial location. As shown in Fig. 1 and Fig. 2, the timing of the distortion to the distribution, as evidenced by the two-component fit, is well correlated with the period of rf application. The temperature of the hot edge ions increases as the amount of rf power is increased. This edge heating of ions has been observed under many plasma conditions: during upper-, lower-, and double-null configurations, in deuterium and helium fueled discharges, at antenna phasings to produce waves with toroidal wave numbers of 3.5, 7, and 14 $m^{-1}$, and at various values of plasma current and toroidal magnetic field.

Fig. 6 shows the variation of ion temperature and velocity, $T_i$ and $v$, of the hot and cold components, as the amount of rf power that is applied to the plasma is increased. Under normal conditions during ohmic heating of the plasma, a reasonable ion temperature for $He^+$ is on the order of the ionization potential for $He^+$, which is ∼54 eV[18]. The hot and cold helium poloidal temperatures at the highest rf input power are ∼500 eV and ∼ 50 eV. The presence of two apparently disparate populations of $He^+$ ions can be reconciled by considering the time scales of relevant processes. These two populations of helium ions would thermalize in ∼ 10 ms, which is much longer than the ionization time scale, ∼ 100 $\mu$s. Light from both populations (hot and cold) would be readily observed, since the emission time scale is ∼ 1 ns.

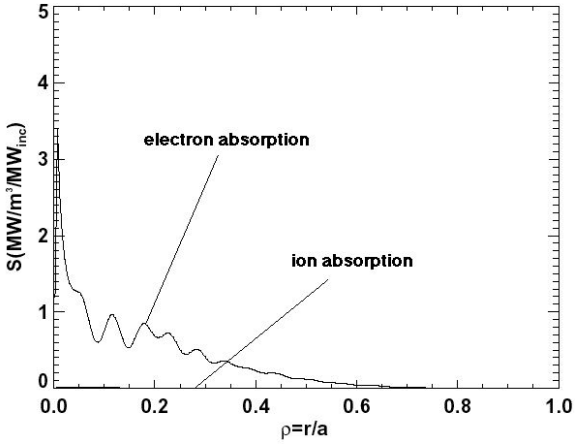


FIG. 4: TORIC code calculations of the predicted power deposition on electrons and helium ions for a launched 30 MHZ HHFW in NSTX. Within this linear treatment, no ion heating is expected in either the plasma core or edge.

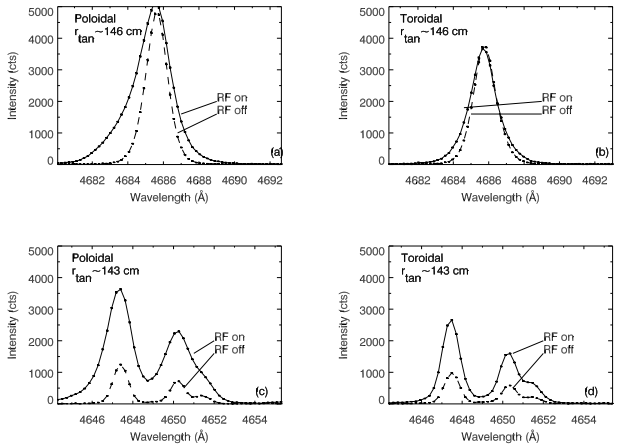


FIG. 5: Spectra from Shot 112310 during adjacent 10 ms time slices (centered on 425 and 435 ms), showing the difference in the $He^+$ (a) poloidal view and (b) toroidal view, and the $C^{2+}$ triplet (c) poloidal view and (d) toroidal view, when HHFW rf heating is applied to the plasma. Rf heating (2.8 MW) ends at 430 ms. Error bars indicate statistical uncertainty.

These time scales allow for the observation of the hot $He^+$ and hot $C^{2+}$ transient states, which are excited by the rf, observed, then promptly ionized. Thermalization presumably occurs among the fully stripped ions.

## III. IBW HEATING

The launched HHFW is not expected to interact directly with the plasma ions. In the region where the ion heating is evident the launched wave is at the $27^{th}$ harmonic of the edge helium ion cyclotron frequency, and at the $41^{st}$ of carbon. However, hot edge ions are observed

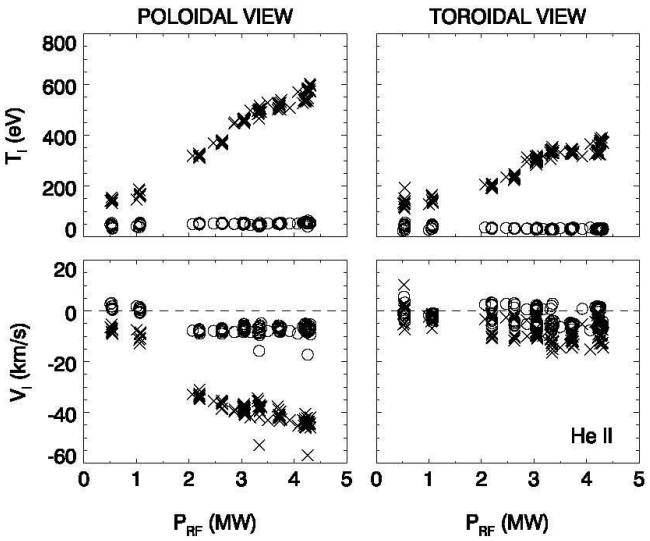


FIG. 6: The temperature of the "hot" helium component (×) scales with $P_{RF}$, whereas the temperature of the "cold" component (o) is not effected by the amount of rf power applied to the plasma. $He^+$ data from Shots 110133-110145 are shown. In the toroidal view, a positive velocity is in the same direction as the plasma current but in the opposite direction to the toroidal magnetic field, while in the poloidal view a positive velocity is downward on the outboard midplane, which is in the same direction as the poloidal magnetic field.

by the ERD. A feature of the ERD is that it has simultaneous toroidal and poloidal views of the plasma edge. Both views observe elevated ion temperatures in the edge, but the poloidally measured temperature is consistently higher than the toroidally measured temperature for a given rf input power. Accounting for the pitch of the magnetic field line ($\sim 28^o$ as calculated by EFIT equilibrium reconstructions[19]), this temperature difference suggests an anisotropy between the perpendicular and parallel edge ion temperatures. In particular, the ERD measurements indicate an enhanced energy content in the perpendicular ion distribution, as shown in Fig. 8.

Ion Bernstein Wave (IBW) heating has been identified as a probable heating mechanism consistent with these observations. Through nonlinear, three-wave coupling the launched HHFW undergoes parametric decay into an ion cyclotron quasi-mode (ICQM) and an IBW[20]. This parametric decay is calculated to occur in the outer 10 cm of the plasma. Power would predominantly go into the most abundant ions: fully stripped $He^{2+}$, but would also heat $C^{6+}$ which has the same cyclotron frequency. The cyclotron resonances for lower charge state ions, $He^+$ and $C^{3+}$, which are also abundant in the edge, are encountered earlier by the HHFW as it moves radially inward, and some power would be deposited in those ions (and even lower charge states). In this manner power is parasitically lost from the HHFW (which was expected to heat only core electrons) to IBW's (which heat edge

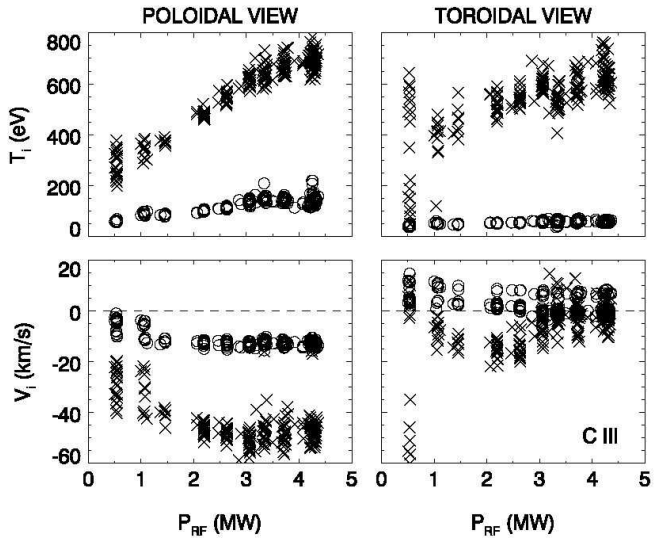


FIG. 7: The temperature of the "hot" carbon component ($\times$) scales with $P_{RF}$, whereas the temperature of the "cold" component (o) is only slightly effected by the amount of rf power applied to the plasma. $C^{2+}$ data from Shots 110133-110145 are shown.

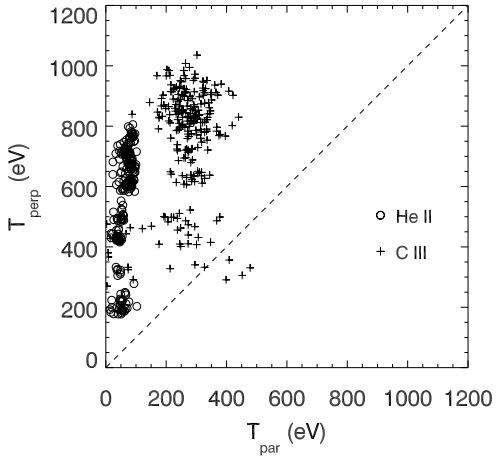


FIG. 8: Perpendicular and parallel edge helium and carbon ion temperatures are calculated from the ERD data, indicating that as the rf power increases the perpendicular $T_i$ exceeds the parallel $T_i$, consistent with IBW heating of the edge ions.

ions). IBW heating affects predominantly the perpendicular ion distribution, consistent with the observation of enhanced poloidal $T_i$ compared to toroidal $T_i$ from the ERD.

The presence of IBW waves in the edge of the plasma has been directly confirmed by Langmuir probe measurements. Fig. 9 shows spectra from a frequency swept Langmuir probe in the edge 2.5 cm radially outward at the midplane from the surface defined by the antenna limiter. When HHFW's are launched by the antenna,

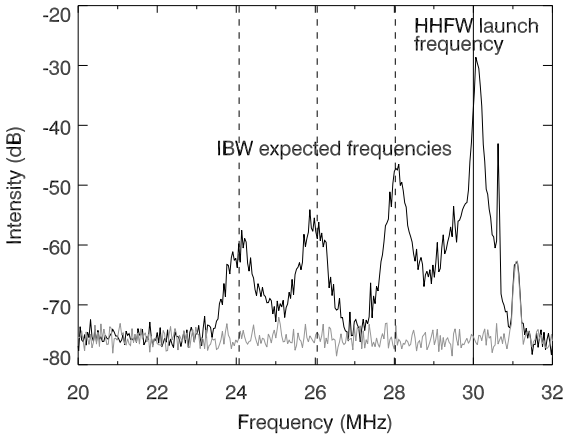


FIG. 9: The frequency spectrum of deuterium shot 112728 (in black) measured by a Langmuir probe near the rf antenna shows the 1 MW launched HHFW (solid vertical line indicates 30 MHz), which has been attenuated with a notch filter by 40 dB, and the detected daughter IBW's (dashed vertical lines indicate the expected IBW frequencies from the first 3 harmonics of the ion cyclotron quasi-mode.) The measured spectrum from shot 112727 (in grey), shows the background level for an ohmic, i.e. no-rf power, discharge. The small peak at 31 MHz is pick-up from a heterodyne network, and is present in both discharges.

sidebands of the launched 30 MHz wave are measured, which correspond to IBW's produced through parametric decay along with low-number harmonics (0, 1, 2, . . .) of the helium ICQM at $\sim$ 2 MHz[21, 22]. As the rf power is increased, more upper and lower sidebands are detected, i.e. corresponding to increasing low-number harmonics of the ICQM.

Parametric decay of the HHFW results in a parasitic loss of energy into IBW's. The amount of power transferred to the IBW's has not been measured directly, but an estimate of the amount of power transferred from the wave can be made by considering the temperature difference between the edge ions and electrons. Though the ions are actually heated by the IBW, it is possible to calculate the amount of power required to maintain the observed temperatures against collisional power transfer to the cooler electrons:

$$Q_i = \frac{3m_e}{m_i}\frac{nk}{\tau_e}(T_e - T_i). \quad (1)$$

Here $m_e$ and $m_i$ are the masses of the electron and the helium ion, $T_e$ and $T_i$ are the electron and hot ion temperatures, $n$ is taken to be the electron density, $k$ is Boltzman's constant, and $\tau_e$ is given by:

$$\tau_e = \frac{3\sqrt{m_e}(kT_e)^{3/2}}{4\sqrt{2\pi}n\lambda e^4}. \quad (2)$$

Here $\lambda$ is the Coulomb logarithm and $e$ is the charge

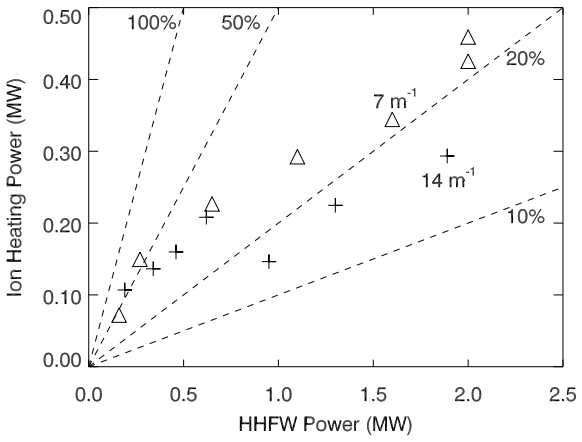


FIG. 10: Estimation of the amount of power absorbed by edge helium ions as the applied rf power is increased for $k_{tor}$ = 7 m$^{-1}$ (△) and 14 m$^{-1}$ (+).

of the electron. This estimate represents a lower bound to the amount of energy directly heating the ions from the wave, since there are other channels which affect the thermal balance of both the ions and electrons. Nevertheless, the result of integrating the collisional heating over the edge (from 140 cm to the outer boundary as determined by equilibrium analysis) is shown in Fig. 10 for two HHFW phasings, $k_{tor}$ = 14 and 7 m$^{-1}$. As the applied HHFW power is increased, the amount of power absorbed by the edge ions increases. Linear fits to the data do not go through the origin, suggesting that the threshold power needed for the parametric decay instability (PDI) is very low, less than 500 kW, and that the PDI is efficient at generating IBW's. Constraining the linear fit to go through the origin indicates that $\sim 22\%$ of the launched HHFW power at 7 m$^{-1}$ is redirected by the PDI into heating edge ions, and $\sim 18\%$ at 14 m$^{-1}$. Again, this represents a lower bound, and only accounts for energy in the thermal ions. As will be discussed later, the PDI is also thought to be responsible for enhancing energetic ions in the tail of the distribution, which represents a further loss of power from the launched HHFW.

## IV. DISCUSSION

The line brightness of $C^{2+}$ is observed to increase by an order of magnitude in the poloidal view (20 cm from the antenna) and by a factor of 3 in the toroidal view (toroidally separated 2 m from the antenna) when rf power is applied. If the antenna is sourcing atoms, this influx of neutral carbon, among other atoms adsorbed to the antenna straps, could charge exchange with the hot, fully stripped $He^{2+}$ plasma ions, rendering them observable to the ERD. The strong increase in signal brightness near the antenna suggests that the antenna itself is likely the source of neutral atoms, though surface waves propagating around the machine may also be responsible in part for sourcing neutral carbon from the carbon-tile covered passive stablizing plates. Unfiltered, visible light camera images of the plasma in the vicinity of the rf antenna confirm the dramatic increase in light emission of plasma adjacent to the antenna.

The two components of the distribution of $He^+$ ions could be due to intrinsic emission of $He^+$ ions (cold component) and to emission of formerly fully stripped $He^{2+}$ ions (hot component), which have undergone charge exchange with neutral atoms. Whereas the cold component maintains an ion temperature that is on the same order as the ionization potential of $He^+$, the hot component could be indicative of the ion temperature of fully stripped $He^{2+}$ in the edge of the plasma, which was heated by the IBW detected by the Langmuir probe. Heating of only the fully stripped ions would not immediately account for the observed, elevated $C^{2+}$ ion temperatures, however. Multiple charge exchange interactions between antenna sourced neutrals and fully striped $C^{6+}$ plasma ions to account for the hot component of $C^{2+}$ emission would be unlikely. Moreover, the hot component of the $C^{2+}$ edge ions is hotter than the hot component of the $He^+$ ions, as shown in Fig. 1 (d) and Fig. 2 (d).

Direct heating of the $He^+$ and $C^{2+}$ from the IBWs is expected, as is heating of all the partially and fully stripped ions in the edge plasma. The ICQM resonances for $C^{2+}$ and $He^+$ and their emission shells are closer to the antenna than for the $He^{2+}$ ions. The majority of the power is deposited in the most abundant ions which have an ICQM resonance in the plasma, i.e. the $He^{2+}$ ions. The side-band frequencies observed on the Langmuir probe are dominated by the $He^{2+}$ resonances, since helium has a much higher relative abundance, especially when compared to the impurity abundance of the various charge states of carbon. Presumably, a Langmuir probe with sufficient frequency resolution would be able to detect side bands from $He^+$ and the charge states of carbon.

The results presented here are another facet of results related to IBW heating. On NSTX, observations have been made of fast-ion tails excited by the application of rf simultaneously with NBI[23, 24]. Recently on Alcator C-Mod observations have been made which indicate that IBW's generated from parametric decay of launched HHFW's are responsible for enhanced ion energies in the edge[25, 26]. And historically, the parametric decay instability of fast waves has been cited as a cause of enhanced ion energies in the edge of ASDEX[27], TEXTOR[28], and JT-60[29]. In all these cases, however, no evidence of edge thermal ion heating was observed, perhaps due to the lack of appropriate diagnostics. In those results neutral particle analyzer (NPA) measurements showed enhanced fast-ions in the high energy tail

of the distribution, and side-bands of the launched fast-wave were measured by probes. In those results, however, once a threshold power was exceeded (typically 500 kW), no additional enhancement of the ion energies was observed. This is contrary to the observations of the ion temperature enhancement seen in the edge of NSTX, where the ion temperature increases as the rf power is increased, and the threshold for edge ion heating is low. However, both the enhanced ion temperature and energy appear to stem from the parametric decay of fast waves into IBW's, and represent channels of power loss for the launched wave.

In Fig. 10 the dependence on parallel wave number is thought to be due to the speed that energy is carried away from the antenna. A smaller $k_{tor}$ corresponds to a larger group velocity of the launched HHFW. At larger group velocity, energy is carried away from the antenna more rapidly, favoring ICQM resonances which are deeper in the edge plasma. A deeper radius of power deposition results in a longer path length to the scrape off layer (SOL) and limiting surfaces. Since the power estimate done in Fig. 10 does not take into account any energy loss channels, the power deposition at larger $k_{tor}$ appears to be less than at shorter $k_{tor}$. This underscores the fact that a more direct measure of the amount of power lost from the launched HHFW is needed, especially a method that is supported by non-linear wave modeling.

## V. CONCLUSION

The rf antenna launched HHFW experiences parametric decay into an IBW and an ICQM in the outer $\sim 10$ cm of NSTX plasma. This decay results in a parasitic loss of power from the HHFW (the majority of which propagates to heat core electrons) into IBW's (which heat the perpendicular distributions of edge ions.) The IBW's theoretically transfer energy to all ion species and all charge states ($He^{+}$, $He^{2+}$, $C^{+}$, $C^{2+}$, . . .) but the majority of the power is absorbed by the most abundant edge ions. The presence of the IBW's is confirmed by Langmuir probe measurements. The hot edge ions are readily observed by a new edge diagnostic on NSTX. The ERD has simultaneous views, which indicate a higher poloidal than toroidal ion temperature in the edge. At the EFIT calculated magnetic field pitch of these plasmas, this anisotropy is consistent with enhanced perpendicular ion temperatures, as expected from IBW heating. This parametric decay is not fundamentally restricted by the rf antenna phasing or wave number, and edge ion heating has been observed in NSTX under all conditions whenever HHFW rf power is applied.

## ACKNOWLEDGEMENTS

The authors wish to recognize the many contributions of the NSTX group and collaborators at Oak Ridge National Lab. Thanks especially to Steve Sabbagh of Columbia University for providing the EFIT reconstructions, and Benoit LeBlanc of PPPL for Thomson scattering data. This research was supported by the U.S. D.O.E. under contract: DE-AC02-76CH03073.

* Electronic address: tbiewer@pppl.gov

[1] J. Spitzer, M. Ono, M. Peng, D. Bashore, T. Bigelow, A. Brooks, J. Chrzanowski, H. M. Fan, P. Heitzenroeder, T. Jarboe, *et al.*, Fusion Technology **30**, 1337 (1996).
[2] E. Strait, *et al.*, Phys. Rev. Lett. **75**, 4421 (1995).
[3] I. Hutchinson, R. Boivin, F. Bombarda, P. Bonoli, S. Fairfax, C. Fiore, J. Goetz, S. Golovato, R. Granetz, M. Greenwald, *et al.*, Phys. Plasmas **1**, 1511 (1994).
[4] The JET Team, in *Proc. 16th Int. Conf. Fusion Energy, Montreal, Canada, 1996* (IAEA, 1997), vol. 1, p. 487.
[5] N. A. Uckan and the ITER Group, *ITER physics design guidelines: 1989* (IAEA, Vienna, 1990).
[6] H. Matsumoto, P. Barabaschi, and Y. Murakami, Fusion Science and Tech. **40**, 37 (2001).
[7] D. M. Meade, Comments on Plasma Phys. Controlled Fusion, Comments on Modern Phys. **2**, 81 (2000).
[8] M. Ono, Phys. Plasmas **2**, 4075 (1995).
[9] R. Majeski, J. Menard, D. Batchelor, T. Bigelow, M. D. Carter, M. Finkenthal, E. F. Jaeger, B. Jones, R. Kaita, T. K. Mau, *et al.*, in *Radio Frequency Power in Plasmas–Thirteenth Topical Conference, Annapolis, MD* (AIP Press, New York, 1999), p. 296.
[10] T. M. Biewer, R. E. Bell, J. R. Wilson, and P. M. Ryan, Phys. Rev. Lett. **submitted** (2004).
[11] Y.-K. Peng and D. Strickler, Nuclear Fusion **26**, 769 (1986).
[12] B. P. LeBlanc, R. E. Bell, D. W. Johnson, D. E. Hoffman, D. C. Long, and R. W. Palladino, Rev. Sci. Instrum. **74**, 1 (2003).
[13] J. R. Wilson, R. E. Bell, S. Bernabie, M. Bitter, P. Bonoli, D. Gates, J. Hosea, B. LeBlanc, T. K. Mau, S. Medley, *et al.*, Phys. Plasmas **10**, 1733 (2003).
[14] T. M. Biewer, R. E. Bell, R. Feder, D. W. Johnson, and R. W. Palladino, Rev. Sci. Instrum. **75**, 650 (2004).
[15] M. Brambilla, Plasma Phys. Control. Fusion **44**, 2423 (2002).
[16] T. M. Biewer, R. E. Bell, D. S. Darrow, and J. R. Wilson, in *Radio Frequency Power in Plasmas–Fifteenth Topical Conference, Moran, WY* (AIP Press, New York, 2003), p. 193.
[17] T. M. Biewer, R. E. Bell, P. M. Ryan, and J. R. Wilson, in *31st European Physical Society Conference on Plasma Physics, London* (ECA, 2004), vol. 28G, pp. P–2.198.
[18] A. R. Striganov and N. S. Sventitskii, *Tables of Spectral Lines of Neutral and Ionized Atoms.* (Plenum Press, 1968).
[19] L. L. Lao, H. S. John, R. D. Stambaugh, A. G. Kellman, and W. Pfeiffer, Nuclear Fusion **25**, 1611 (1985).
[20] M. Porkolab, Eng. Fusion and Design **12**, 93 (1990).

[21] F. Skiff, M. Ono, and K. L. Wong, Phys. Fluids **27**, 1051 (1984).
[22] F. N. Skiff, K. L. Wong, and M. Ono, Phys. Fluids **27**, 2205 (1984).
[23] A. L. Rosenberg, Ph.D. thesis, Princeton University (2003).
[24] A. L. Rosenberg, J. E. Menard, J. R. Wilson, S. S. Medley, R. Andre, C. K. Phillips, D. S. Darrow, B. P. LeBlanc, M. H. Redi, N. J. Fisch, *et al.*, Phys. Plasmas **11**, 2441 (2004).
[25] J. C. Rost, M. Porkolab, and R. L. Boivin, Phys. Plasmas **9**, 1262 (2002).
[26] J. C. Rost, R. L. Boivin, M. Porkolab, J. C. Reardon, and Y. Takase, in *Radio Frequency Power in Plasmas–Twelfth Topical Conference, Savannah, GA* (AIP Press, New York, 1997), p. 85.
[27] R. V. Nieuwenhove, G. V. Oost, J. M. Noterdaeme, M. Brambilla, J. Gernhardt, and M. Porkolab, Nuclear Fusion **28**, 1603 (1988).
[28] G. V. Oost, R. V. Nieuwenhove, R. Koch, A. M. Messiaen, P. E. Vandenplas, R. R. Weynants, K. H. Dippell, K. H. Finken, Y. T. Lie, A. Pospieszczyk, *et al.*, Eng. Fusion and Design **12**, 149 (1990).
[29] T. Fugii, M. Saigusa, H. Kimura, M. Ono, K. Tobita, M. Nemoto, Y. Kusama, M. Seki, S. Moriyama, T. Nishitani, *et al.*, Eng. Fusion and Design **12**, 139 (1990).